Investigation of Pole-to-Pole Performances of Spaceborne Atmospheric Chemistry Sensors with the NDSC

JEAN-CHRISTOPHER LAMBERT, MICHEL VAN ROOZENDAEL, MARTINE DE MAZIÈRE, AND PAUL C. SIMON

Institut d'Aéronomie Spatiale de Belgique, Brussels, Belgium

JEAN-PIERRE POMMEREAU, FLORENCE GOUTAIL, AND ALAIN SARKISSIAN

Service d'Aéronomie du CNRS, Verrieres-le-Buisson, France

JAMES F. GLEASON

NASA/Goddard Space Flight Center, Greenbelt, Maryland

(Manuscript received 12 September 1997, in final form 27 May 1998)

ABSTRACT

Spaceborne atmospheric chemistry sensors provide unique access to the distribution and variation of the concentration of many trace species on the global scale. However, since the measurements and the retrieval algorithms are sensitive to a variety of instrumental as well as atmospheric sources of error, they need to be validated carefully by correlative measurements. The quality control and validation of satellite measurements on the global scale, as well as in the long term, is one of the goals of the Network for the Detection of Stratospheric Change (NDSC). Started in 1991, at the present time the NDSC includes five primary and two dozen complementary stations distributed from the Arctic to the Antarctic, comprising a variety of instruments such as UV–visible spectrometers, Fourier transform infrared spectrometers, lidars, and millimeter-wave radiometers.

After an overview of the main sources of uncertainty which could perturb the measurements from space, and of the ground-based data provided by the NDSC for their validation, this paper will focus, as an example, on the measurement of total ozone by Earth Probe Total Ozone Mapping Spectrometers (TOMS), ADEOS TOMS and *ERS-2* Global Ozone Monitoring Experiment (GOME) and their validations. The data recorded between summer 1996 and April 1997 by 16 Système d'Analyse par observations zénithales (SAOZ)/UV–visible spectrometers distributed over a range of latitudes from the Arctic to the Antarctic, and by Dobson and Brewer spectrophotometers operating at selected sites of the NDSC alpine and Antarctic stations, are used to investigate the solar zenith angle (SZA) dependence, the dispersion, the time-dependent drift, and the possible differences of sensitivity of the space-based sensors. Although the comparison demonstrates an excellent agreement to within $\pm$2%–4% between all space- and ground-based instruments at northern middle latitudes, it also reveals significant systematic features, such as a SZA dependence with TOMS beyond 80°, a seasonal SZA dependence with GOME beyond 70°, a systematic bias of a few percent between satellite and SAOZ observations of low ozone columns in the southern Tropics, a difference in sensitivity to ozone between the GOME and ground-based sensors at high latitudes, and an interhemispheric difference of TOMS with the ground-based observations.

1. Introduction

The global composition of the earth's atmosphere is changing due to the increasing anthropogenic release of chemically and radiatively active species. A better knowledge of the global composition of the atmosphere as well as its long-term evolution are urgently needed to assess current and future changes. Only remote sensing from a satellite platform can provide the required continuous measurements of relevant atmospheric trace species on the global scale. However, as demonstrated on several occasions in the past, satellite observations are subject to time-dependent drifts. They are of limited sensitivity in the lower stratosphere and the troposphere because of clouds and other physical limitations, such as line broadening. Before being used for a specific scientific application, the relevance of satellite measurements must be investigated carefully by means of intensive coordinated geophysical validation campaigns. The primary purpose of these campaigns is to verify that the data provided by the satellite experiment do respond to spatial, temporal, and quality requirements specific to the application for which the experiment has been designed. In particular, the accuracy and

Corresponding author address: Jean-Christopher Lambert, Institut d'Aéronomie Spatiale de Belgique (IASB-BIRA), Avenue Circulaire 3, B-1180 Bruxelles, Belgium.
E-mail: lambert@bira-iasb.oma.be

precision of these data must be assessed over the whole relevant spatial domain and vertical range during the entire mission. In addition, satellite observations are not continuous since they depend strongly on space policies of the various nations. The link needed between sensors operating on different platforms must be studied.

The performance of an atmospheric sensor can be investigated by analyzing its measurements with respect to high quality correlative observations. In turn, the satellite data provide an insight into ground-based measurements and point out key issues for the improvement of ground-based remote sensing techniques. The independent calibration and validation of satellite experiments is precisely one of the main goals of the high quality remote-sounding research stations of the Network for the Detection of Stratospheric Change (NDSC). The NDSC started operating in 1991, under the auspices of the United Nations Environment Program, the International Ozone Commission of the International Association of Meteorology and Atmospheric Physics, and the World Meteorological Organization (WMO). It is a major contributor to the WMO's Global Ozone Observing System (GO_3OS) within the framework of the Global Atmosphere Watch. The NDSC consists of about 17 sites distributed in five primary stations (Arctic, Alpine, Hawaii, New Zealand, Antarctic) and two dozen complementary sites. By means of various observation techniques, each NDSC primary station provides total column measurements of ozone, nitrogen dioxide, and other key constituents, such as NO_y, ClO_y, or CH_4, as well as vertical distributions of ozone, temperature, water vapor, ClO, and aerosols. In particular, total ozone is monitored with UV–visible spectrometers, with Dobson and Brewer spectrophotometers, and with Fourier transform infrared spectrometers (FTIR). Complementary NDSC sites are equipped with a limited number of instruments validated in the same way as those of the primary stations. In the framework of the NDSC, 17 SAOZ (Système d'Analyse par Observations Zénithales) and other NDSC-qualified UV–visible spectrometers have been deployed at primary and complementary sites, constituting the so-called SAOZ/UV–visible network. Altogether, these instruments allow twice-daily observations of ozone and nitrogen dioxide column amounts all over the world, from the Arctic to Antarctica. The activities of the SAOZ/UV–visible network are supported by national funding from several European countries and by the Environment Programme of the European Commission (DGXII).

Since the beginning of their operation, both the NDSC and the SAOZ/UV–visible network have demonstrated their efficiency and complementarity in satellite validation research. Their contribution has been valuable in assessing the performances of the series of NASA's Total Ozone Mapping Spectrometers (TOMS), of the instruments on board the *Upper Atmosphere Research Satellite* (*UARS*), and of the current ESA Global Ozone Monitoring Experiment (GOME). Those networks should also play a major role in the validation and interpretation of data of future missions such as the ESA's Environment Satellite (ENVISAT-1). Based on the heritage of the GOME, TOMS, and *UARS* validation, the main purpose of the present paper is to give an overview of the capabilities and complementarity offered by both ground-based networks for investigating the pole-to-pole performances of space-based sensors for the measurement of atmospheric composition in general and, more specifically, total ozone. The paper starts with a general introduction of satellite remote sensing devoted to the chemistry of the lower and middle atmosphere, highlighting several sources of uncertainty of measurements from space. In section 3, an overview of the potential of the NDSC for validating and interpreting satellite total ozone observations is given. In section 4, a brief review of its potential for the validation of the measurements of other species is provided. Finally, the concept will be illustrated in section 5 by the example of a preliminary evaluation of total ozone measured from space by the Earth Probe TOMS, the *ADEOS* TOMS, and the *ERS-2* GOME, using ground-based observations associated with the NDSC and the SAOZ/UV–visible network.

2. Spaceborne sensors

Current and future instruments in orbit are expected to provide information on major scientific issues related to the photochemistry and dynamics of the lower and middle atmosphere. Of primary concern are the budgets of odd oxygen, nitrogen, chlorine, and hydrogen families and of water vapor; the partitioning between specific molecules of these families; methane oxidation; the strong springtime ozone depletion at high latitudes; and the long-term decrease of the ozone column at both high and middle latitudes. Target species of principal importance are ozone, nitrogen compounds, chlorine and bromine families, HO_2, OH, HCHO, and CH_4, as well as aerosols and temperature.

Most of the space-based optical remote sensing techniques are based on two main viewing geometries: the limb and the nadir viewing. Both require an accurate knowledge of the spacecraft position and attitude. When sounding the limb of the atmosphere, a sensor observes the radiation leaving the atmosphere tangentially. An accurate measurement of the solar elevation angle is therefore essential, together with a relatively large amount of absorber or emitter in the line of sight. In occultation mode, the vertical resolution may be high, but a relatively poor horizontal resolution results. Clouds can alter significantly the radiation field and may perturb the measurement around the tropopause and below. For measurements in solar occultation mode (i.e., in absorption when the sun rises or sets), the enhanced light path of the limb geometry combines with large signals to allow the detection of weak absorbers, but the observation geometry yields poor spatial and tem-

poral coverage. In addition, the concentration of many relevant atmospheric constituents changes rapidly during twilight, making their retrieval more difficult and less accurate. Stellar occultation can lead to much better spatial and temporal coverage. But other problems arise, such as scintillation because of refraction within thin layers in the atmosphere or wavelength registration uncertainties of the source spectral features when its spectrum is not structured enough. When pointing in the nadir direction, a sensor observes radiation emitted or scattered by the atmosphere and the earth's surface. The method is less sensitive to inaccuracies in the direction of observation and allows high horizontal resolution but limited vertical resolution. At small solar zenith angles (SZA), spectral signatures from weak absorbers or emitters may be under the detection threshold. Clouds perturb the radiation field and mask the troposphere. In the infrared spectral region, radiation detected in the nadir includes features due to atmospheric constituents superimposed on the background thermal signal of the earth's surface.

The performance of optical instruments is known to degrade with time, especially in the space environment. Changes in the properties of optical elements (e.g., degradation of the diffuser or contamination of optical surfaces), in the response of the detectors and their electronics, and from thermal and mechanical phenomena are a few causes of this instrumental degradation. Wavelength registration and absolute signal level calibration are also subject to time-dependent drifts that may alter the accuracy of the retrieved atmospheric abundances.

Column and profile retrievals are sensitive to uncertainties in input parameters in the spectral analysis and in the radiative transfer model, such as laboratory absorption cross sections and a priori assumptions in the composition and properties of the atmosphere or the earth's surface. In particular, uncertainties due to features exhibiting a seasonal variation (e.g., vertical distributions of temperature and of radiatively active species, snow or ice cover, tropopause height) combine with solar zenith angle dependences, resulting in periodic, systematic errors. Clouds and aerosols can modify the albedo and the radiation field dramatically, and the determination of their coverage and properties is critical. The impact of polar stratospheric clouds and volcanic aerosols has already been demonstrated to perturb significantly the retrieval of total ozone from the earth's radiance measurements in the ultraviolet Huggins band (Torres et al. 1992; Bhartia et al. 1993). Tropospheric clouds prevent spaceborne sensors from seeing the lower part of the atmosphere and require the use of climatological information about constituents below clouds. Even under clear-sky conditions, uncertainties in the radiation field arise from large uncertainties in the spectral properties of the surface, which, in addition, may change significantly as a function of land use, vegetation, and season.

3. Ground-based sensors for total ozone

Total ozone is monitored at NDSC stations by Dobson and Brewer spectrophotometers, UV–visible spectrometers, and FTIR spectrometers. In order to ensure the quality of the measurements, most of the instruments are routinely calibrated and regularly compared. Blind intercomparison campaigns are also organized through the NDSC. This section describes the main ground-based total ozone sensors, their mutual consistency, and their capabilities, limitations, and complementarity for the validation of satellite data.

a. Ultraviolet spectrophotometers

The column abundance of ozone can be derived from differential absorption measurements in the ultraviolet Huggins band, where ozone exhibits strong absorption features. Based on this method, the *Dobson* instrument consists of a double prism monochromator (Dobson 1957). Its principle relies on the measurement of the ratio of the direct sunlight intensities at standard wavelengths. The most widely used wavelength combination, recommended as the international standard, is the two pairs of wavelengths referred to as the AD pair (305.5–325.4 nm; 317.6–339.8 nm) (Komhyr et al. 1993). Started in the 1950s, the international network of more than 100 Dobson spectrophotometers forms the world's primary total ozone monitoring network and is a key component of the WMO's Global Ozone Observing System. The *Brewer* grating spectrophotometer is similar in its principle to the Dobson but with an improved design that is fully automated (Kerr et al. 1983). The ozone column abundance is derived from a combination of four wavelengths between 310 and 320 nm. A fifth wavelength is used to determine the SO_2 column abundance. About 100 Brewers operate as part of the GO_3OS. A few Dobson and Brewer spectrophotometers are recommended at primary NDSC sites.

During international intercomparison campaigns, Dobson instruments can be adjusted to agree within 0.3%–1% (Basher 1994). The long-term agreement between Dobson and Brewer total ozone at high and moderate sun elevation—that is, at low and moderate air mass—is generally better than 1%, while day-to-day fluctuations in the difference are usually small, on average less than $\pm 1.5\%$ (e.g., Kerr et al. 1988; De Backer and De Muer 1991). At low sun elevation, mean differences of $\pm 5\%$ are reported (Nichol and Valenti 1993). Dobson and Brewer instruments might suffer from long-term drift associated with calibration changes for which corrections are needed. Calibration errors also generate a relative airmass dependence. An additional problem arises at low solar elevation, where the contributions of diffuse and of direct radiation are of the same order of magnitude and vary with the aerosol load. The contribution of short wavelengths is relatively larger in the diffuse component, leading to an erroneous decrease in

measured ozone abundance as the airmass increases (Josefsson 1992). Internal scattering within the spectrophotometer also increases at high SZA. According to Van Roozendael et al. (1998a), the temperature dependence of the ozone absorption coefficients used in the Dobson and Brewer retrievals might account for a seasonal variation of $\pm 0.9\%$ at Payerne, Switzerland (46.5°N), of $\pm 1.7\%$ at Sodankylä, Finland (67.4°N), and for a systematic offset smaller than 1%. The effect can dramatically increase in extremely cold conditions such as those met in the winter polar vortex, where stratospheric temperature can reach that associated with the formation of polar stratospheric clouds (PSC) of type I (195 K) and type II (189 K). Ozone measurements in the ultraviolet can be affected by interfering species, such as SO_2 and NO_2 (Kerr et al. 1988 and references therein). The effect of SO_2 on Dobson data is an erroneous increase of total ozone by 0.3% on average, depending on the location of the station. Furthermore, according to De Muer and De Backer (1992), the long-term trend of SO_2 generally ascertained in European and North American urban areas would induce, if not properly taken into account, a fictitious Dobson total ozone trend, for example, of -1.69% per decade in urban stations such as Uccle, Belgium (50.5°N). The wavelengths used in the Brewer ozone measurement are chosen to avoid interferences by SO_2. Interferences by NO_2 may be neglected for both Dobson and Brewer measurements, except during strong NO_2 tropospheric pollution events, which can produce an erroneous increase of total ozone by 0.6% in extreme cases. Built up from quasi-simultaneous direct sun and zenith-sky measurements, a sky chart can be used to derive total ozone from Dobson and Brewer zenith-sky readings. This method is useful for obtaining data in cloudy conditions or in regions frequently overcast, like Antarctica. However, a sky chart is known to be less accurate, depending, among other things, on the optical properties of the cloud cover (Dahlback 1995). Moreover, due to the degradation of accuracy at low solar elevation and the mostly cloudy conditions in winter, sky charts at polar latitudes would not be suitable in winter (Taalas and Kyrö 1992).

In summary, with well-maintained Dobson and Brewer instruments, the error of individual total ozone measurements may be estimated to be within 0.3%–1% under conditions of high sun, clear sky, and low ozone. Under less favorable conditions, the error budget analysis concludes to a 2%–3% accuracy at high and moderate sun elevation (typically beyond 20°), and about 5%–7% at lower sun elevation and in polar winter. This error budget includes the temperature dependence of the UV absorption coefficients, which might account for an erroneous seasonal variation of $\pm 0.9\%$ at middle latitudes and $\pm 1.7\%$ at the Arctic polar circle, and for a systematic offset smaller than 1%. Uncertainties related to calibration errors, temperature dependence, aerosols, and interfering species depend on the location of the station, on the vicinity of pollution sources, and on the detailed history of the instrument calibration.

b. Ultraviolet–visible zenith-sky spectrometers

Several trace constituents, such as ozone, NO_2, O_4, H_2O, BrO, and OClO, can be detected from UV–visible zenith-sky observations at twilight (e.g., Brewer et al. 1973; Noxon et al. 1979; Solomon et al. 1987; Pommereau and Goutail 1988). Based on the technique pioneered by Dobson (1957), the retrieval method, referred to as the Differential Optical Absorption Spectroscopy (DOAS), consists of studying the narrow absorption features of the species, after removal of the broadband signal due to scattering processes. A differential optical thickness is calculated as the logarithm of the ratio between the actual zenith-sky spectrum and a reference recorded at lower SZA. Column densities along the optical path, or apparent slant columns, are derived by an iterative least squares procedure, fitting the observed differential optical thickness with high-resolution differential absorption cross sections measured in the laboratory and convolved with the instrument slit function. Apparent slant columns are converted into vertical columns using a geometrical enhancement factor, or air mass factor (AMF). This AMF is calculated with a radiative transfer model assuming vertical distributions of the target absorber and of the atmospheric constituents controlling the path of the solar radiation into the atmosphere.

Based on this technique, about 25 UV–visible DOAS spectrometers constitute the backbone of the NDSC for total ozone and nitrogen dioxide monitoring. Among them, the SAOZ grating spectrometer (Pommereau and Goutail 1988) derives apparent slant column amounts of ozone in the Chappuis band (between 470 and 540 nm) and of NO_2 in the 406–526-nm spectral window. Slant columns retrieved from a real-time spectral analysis at the station are converted into preliminary total vertical columns by the use of a standard AMF calculated for 60°N (Sarkissian et al. 1995a). Together with two DOAS spectrometers designed, respectively, at the Belgian Institute for Space Aeronomy (Van Roozendael et al. 1995) and at the Norwegian Institute for Air Research, 17 SAOZ instruments are currently performing network operations from the Arctic to the Antarctic.

When the uncertainty of the high-resolution ozone absorption cross sections and the one sigma confidence level of the least squares fit calculated for each spectrum are taken into account, the overall accuracy of the SAOZ ozone apparent slant column amounts is better than 2%. Wavelength calibration changes should not exist for SAOZ instruments since they are self-calibrated permanently by reference to the solar Fraunhofer absorption lines. As shown by Brion et al. (1993), the temperature dependence of the ozone cross sections in the visible is not significant ($<1\%$). At shorter wavelengths, the temperature dependence reported by Burkholder and

Talukdar (1994) is too small to have a significant effect on atmospheric observations with the DOAS method. The main sources of uncertainty on the vertical column are associated with the AMF. The zenith-sky AMF is sensitive to the altitude of the site; to the vertical distribution of pressure and temperature, which controls the scattering geometry; and to the ozone density profile. Short-term fluctuations of these parameters might account for a $\pm 1\%$ scatter in the retrieved total ozone (Lambert et al. 1996a). For real-time SAOZ data based on the standard AMF calculated at 60°N, seasonal change of the ozone profile and scattering geometry introduces a systematic seasonal bias of about 5%–6% amplitude at 67°N, 3%–4% at 44°N, and negligible in the Tropics (Høiskar et al. 1997; Van Roozendael et al. 1998a; Denis et al. 1995). The use of the standard SAOZ AMF also introduces an average latitudinal dependence of -3% at 67°N to $+2.8\%$ at the Tropics, due to the latitudinal drift in altitude of the ozone maximum. Another source of uncertainty of the AMF arises from the increasing tropospheric contribution during strong pollution events. AMFs are also affected by changes in the effective optical path of the scattered light. Tropospheric multiple scattering, generated by fog, thick clouds, or snow showers, can enhance the tropospheric light path. This enhancement increases the absorption by ozone and interfering species, such as O_4 and H_2O, resulting in a bias in the retrieved ozone (Van Roozendael et al. 1994). According to Van Roozendael et al. (1998a), this contribution does not exceed 1% on average at midlatitudes if erroneous data are rejected after detection by adequate criteria. The impact of aerosols depends largely on the altitude distribution of both ozone and the aerosols (Sarkissian et al. 1995b). Short-term variations of the background aerosol load should not affect the twilight AMF by more than $\pm 0.5\%$. The reduced stratospheric aerosol layer observed in the Antarctic vortex in winter might increase the actual AMF by 1%. The effect is expected to be more significant with the strong aerosol load released by major volcanic eruptions and with dense PSCs of type II. Finally, a constant offset in the retrieved total ozone can result from the uncertainty of the determination of the residual ozone amount in the reference spectrum, depending on the method used to estimate the residual ozone. This offset can be significantly reduced with methods based on an ozonesonde measurement or on a reference spectrum recorded in the direct sun mode (Vaughan et al. 1997; Lambert et al. 1996a).

At the Tenth WMO Dobson Intercalibration Campaign held at Arosa in July–August 1995 (WMO 1995), the mean bias between the Dobson and Brewer #40 was found to be less than 1%, and less than 1.6% with SAOZ #13 (operated at the same site for intercomparison purposes). Long-term comparisons of SAOZ total ozone with Dobson or Brewer collocated observations at midlatitudes show an agreement within 0%–2.4% with a scatter of about 5% (Van Roozendael et al. 1998a; Lambert et al. 1996a, 1998a). NDSC and European field intercomparison campaigns of UV–visible spectrometers were held in May 1992 at Lauder in New Zealand (Hofmann et al. 1995), in September 1994 at Camborne in the United Kingdom (Vaughan et al. 1997), and in June 1996 at the Observatoire de Haute Provence in France (Roscoe et al. 1998). At Camborne, the difference between four SAOZ and other DOAS spectrometers was smaller than 3% for total ozone, as well as with the collocated Dobson and integrated ozonesonde profiles. Similar conclusions have been reached after the NDSC intercomparison of 16 ground-based ozone sensors in 1996 in France.

In summary, with a well-maintained UV–visible DOAS spectrometer, the error in individual total ozone measurements may be estimated to be within 2%–3.5%. This error budget includes the impact of (i) uncertainties on the ozone absorption cross sections and measurement noise ($\pm 2\%$ on the slant column), (ii) short-term fluctuations of the ozone profile and scattering geometry ($\pm 1\%$), (iii) tropospheric multiple scattering ($\pm 1\%$), (iv) aerosol effects ($< \pm 0.5\%$), and (v) uncertainties on the ozone residual amount in the reference spectrum ($\pm 1\%$). For real-time data retrieved with the standard SAOZ AMF, seasonal and latitudinal changes of the ozone profile and scattering geometry might account for a latitudinal dependence of -3% at 67°N to $+2.8\%$ at the Tropics, and an erroneous seasonal variation of about 5%–6% at 67°N, 3%–4% at 44°N, and negligible in the Tropics. Aerosol effects are expected to increase significantly after major volcanic eruptions and with the presence of dense PSCs (type II). Finally, the uncertainty of the residual ozone in the reference spectrum can generate an offset up to 3% if not determined by the most accurate methods.

c. Fourier transform infrared spectrometers

A large number of atmospheric trace constituents offer absorption features in the infrared range: ozone, nitrogen compounds, HCl, HF, CO, CH_4, CFCs, and others. By the application of Fourier transform infrared spectroscopy (FTIR), the vertical column of those species can be inferred from high-spectral-resolution measurements of the solar spectrum. FTIR measurements can also be performed using the full moon as an infrared light source (Notholt et al. 1993). An advantage of the FTIR approach is that many species are measured simultaneously. In particular, several suitable unsaturated ozone transitions with minimal overlap by interfering lines are available in the commonly covered infrared spectral region from 2.5 to 12.5 μm. The ozone abundance is retrieved with a multilayer least squares fitting procedure assuming vertical distributions of pressure, temperature, ozone, and possible interfering species. Most of the current FTIR analysis algorithms use the 1992 HITRAN compilation as the spectrometric database (Rothman et al. 1992).

Errors in total ozone arise from uncertainties of sev-

eral percent in spectral parameters such as the absolute ozone line intensities, their Lorentz broadening, and their temperature dependence, and from interferences with other absorbing species. The temperature dependence can be minimized by choosing appropriate lines, while minimization of interferences can be achieved through high spectral resolution and the choice of appropriate spectral microwindows. Optical misalignments generate additional uncertainties in the instrument line shape, which can cause biases of several percent in the retrieved ozone column amount if these effects are not modeled correctly (Zander et al. 1994). FTIR retrievals are also affected by deviations of the actual from the assumed vertical distributions of temperature, pressure, and volume mixing ratios of the target and interfering species (Zander et al. 1994). In particular, this effect seems to be the major source of a 3%–4% systematic seasonal variation between FTIR and other ground-based total ozone observations, as reported by De Mazière et al. (1998a) after five years of comparison between FTIR and SAOZ measurements at the Jungfraujoch, Switzerland (46.5°N), and by Murata et al. (1997) after one year of comparison between FTIR and Dobson observations at Rikubetsu, Japan (43.5°N). Most of the comparison studies also report a systematic underestimation of Dobson, Brewer, and SAOZ total ozone by FTIR observations, for which possible reasons are currently being investigated.

d. Instrument complementarity

Correlative studies relying on the entire Dobson and Brewer datasets have proved to be invaluable for investigating the performances of spaceborne total ozone sensors (e.g., Bhartia et al. 1984). Among other things, this approach yields a statistically significant study of sun-synchronous satellite data due to the good airmass coincidence and the large amount of ground-based data. From the previous sections, it appears clear that the various ozone observation techniques used in the frame of the NDSC provide powerful complementary information for satellite validation and complement the classic Dobson–Brewer approach by extending its capabilities. Altogether, correlative measurements of the NDSC cover a wide range of quality controlled measurements of total columns and profiles of a variety of species and parameters, distributed over a wide range of latitude and season. Direct sun total ozone measurements in the ultraviolet (Dobson, Brewer) and in the infrared (FTIR) yield a very good temporal coincidence with sun-synchronous satellite data. Given a clear sky throughout the day, both direct sun observations can provide information on the short-term variation of the monitored constituents. Under cloudy conditions, Dobson and Brewer measurements are feasible only with the less accurate zenith-sky approach, while FTIR observations are not suitable. Although Dobson and Brewer spectrophotometers are believed to provide the most accurate measurements of total ozone, their accuracy degradation at low sun elevation combines with their temperature dependence, preventing reliable ozone monitoring in wintertime and early springtime polar regions. Observations during the polar night can be performed using the full moon, but this technique is not used on a regular basis. On the opposite, zenith-sky DOAS observations in the visible are possible up to the polar circle throughout the year. Since they are performed always during twilight, when their sensitivity to stratospheric absorbers and their accuracy are the best, they are not sensitive to the SZA. Combined with their generally low sensitivity to clouds and their negligible temperature dependence, their high accuracy at large SZA makes them particularly well suited for satellite validation in polar areas. This advantage is reinforced by the similarity of the stratospheric path of the sunlight observed by ground-based zenith-sky and spaceborne nadir-viewing instruments at twilight (Lambert et al. 1998a), and their good temporal coincidence.

4. Other species and parameters

a. Nitrogen dioxide

UV–visible spectrometers provide the vertical column of nitrogen dioxide at dawn and at dusk. In the SAOZ algorithm, the DOAS fitting procedure is applied in the 406–526-nm spectral window of the spectra (Pommereau and Goutail 1988). Taking into account the 5% uncertainty of the NO_2 absorption cross sections (Merienne et al. 1995) and the 1.5% one sigma confidence level of the least squares fit calculated for each spectrum, the overall accuracy of the SAOZ NO_2 slant total amounts is better than 5% providing the large temperature dependence of the NO_2 cross sections demonstrated by Harwood and Jones (1994) and Coquart et al. (1995) is taken into account. However, the largest uncertainty in the vertical column still remains the AMF, which varies by large factors with the time of the day, the latitude, and the season, and has been difficult to characterize until recently due to the near absence of profile measurements. As mentioned already in section 3, major NDSC field intercomparison campaigns of UV–visible spectrometers also focus on NO_2. As an example, in September 1994 at Camborne, the agreement between the four SAOZ and seven other DOAS NO_2 sensors was within 5% (Vaughan et al. 1997). UV–visible spectrometers of the NDSC and the SAOZ/UV–visible network have been valuable during the maturation of the first public version of the GOME total NO_2 retrieval (GDP 2.0) (Lambert et al. 1996b). They have been used to investigate the integrated stratospheric NO_2 profiles as well, as reported by Cunnold et al. (1991) for the validation of the Stratospheric Aerosol and Gas Experiment (SAGE II) and by Gordley et al. (1996) for that of the *UARS* HALOE dataset. Moreover, height-resolved information on NO_2 can be derived from UV–visible ze-

nith-sky observations (McKenzie et al. 1991; Preston et al. 1997, 1998). This technique could be valuable for identifying the tropospheric component of the total column, a quantity which is extremely variable and to which nadir-viewing geometry is much more sensitive than zenith-sky geometry. For the validation of NO_2 profile measurements from space, ground-based monitoring of height-resolved NO_2 performed on a regular basis will offer a good complementarity with more sporadic UV–visible and infrared balloonborne experiments.

FTIR spectrometric observations cover nearly the complete NO_y family, including NO_2. A comparison study of collocated SAOZ and FTIR total NO_2 observations at the Jungfraujoch has shown a good agreement between the observations of both techniques (De Mazière et al. 1998b). While the zenith-sky visible technique delivers NO_2 morning and evening twilight columns, the FTIR covers the variation of the NO_2 column throughout the day. A combined exploitation of thus both allows the observation of the complete daytime diurnal variation, which may be interesting to compare with satellite observations taken at different SZA.

b. Vertical distribution of ozone

The NDSC combines several techniques for the observation of the ozone vertical distribution. Ozonesondes are generally launched several times a month and sometimes almost daily at particular stations during special events. They record vertical profiles of ozone partial pressure, total pressure, and temperature from the ground up to burst point, typically 30 km, with a vertical resolution of about 100 m. Lidar soundings are performed at each of the five primary NDSC stations several times per week under clear skies, that is, about 200 nights a year in the Alps but much less in Antarctica. Ozone number density is measured by stratospheric lidar from 15 to 45 km with a vertical resolution of 300 m–3 km depending on the altitude and a precision of 2%–5%. Tropospheric lidars can be used for altitude below 15 km. Millimeter-wave radiometers can operate night and day, providing ozone volume mixing ratios integrated over typically 2 h from 25–30 to 70 km, with a vertical resolution of 8–12 km and a corresponding accuracy of 5%–20%. These three ground-based and in situ instruments constitute the backbone of the NDSC ozone profile monitoring. Combining their observations into a composite profile, comparisons with satellite measurements can be carried out over the complete vertical range from the ground up to 70 km. The various measurement times permit the comparison of ground-based and space-based studies of features such as the diurnal variability of mesospheric ozone (Ricaud et al. 1996). If degraded to the vertical resolution of the satellite instrument by means of its averaging kernels, profile observations at high vertical resolution (ozonesonde and lidar) can be valuable in testing the satellite retrieval algorithms. Finally, information on the vertical distribution of ozone is also derived from Dobson and Brewer observations of the Umkehr effect (Götz et al. 1934) and from infrared spectra recorded by ground-based FTIR spectrometers (e.g., Menzies and Chahine 1974; Abbas et al. 1978; Pougatchev et al. 1995).

c. Other products

Many key constituents other than ozone and NO_2 are monitored at NDSC sites. Halogen compounds such as BrO and OClO are detected by UV–visible DOAS. Preliminary ground-based validation of the GOME BrO over Greenland has already been reported by Hegels and Perner (1996). FTIR spectroscopy provides vertical column amounts of many halogen and nitrogen compounds and other relevant molecules such as HCl, HF, HNO_3, NO, N_2O, $ClONO_2$, CH_4, and CO. Vertical profiles of several trace species, such as HF and HCl, can also be derived from ground-based FTIR observations (Liu et al. 1996). A correlative analysis of the integrated total column, seasonal variation, and annual trend of HCl and HF measured by HALOE on board *UARS* has been carried out using FTIR observations at the Alpine and Hawaii NDSC stations (Russell et al. 1996a,b). Temperature vertical distributions as well as semidiurnal and diurnal tides observed by the instruments on board *UARS* have been validated with lidar temperature measurements at several NDSC sites (Hervig et al. 1996; Keckhut et al. 1996). Millimeter wave radiometers provide useful height-resolved information on ClO (from about 25 to 45 km, depending on latitude) and H_2O (from about 20 to 80 km). Measurements of the spectral distribution of UV radiation received at the ground are performed by a variety of instruments, such as spectroradiometers (e.g., McKenzie et al. 1992) and multichannel filter radiometers (Dahlback 1996), from which total ozone can also be derived. Finally, information on aerosol content can be obtained by aerosol lidar and backscattersonde.

5. Example: Total ozone from ground-based and orbiting sensors

Comparisons with ground-based observations have played a major role in the validation and the improvement of two spaceborne ozone monitoring instruments: NASA's TOMS and ESA's GOME. After a short description of the TOMS and GOME missions as well as a summary of the previous validation activities carried out with ground-based networks, total ozone measured from summer 1996 through April 1997 by the *ERS-2* GOME, the *Earth Probe* TOMS, and the *ADEOS* TOMS is compared to correlative ground-based observations associated with the NDSC. The ground-based stations and instruments contributing to this preliminary study are listed in Table 1. Investigations focus on the SZA dependence, the seasonal and latitudinal drifts, the dis-

TABLE 1. Ground-based stations and instruments contributing to the present analysis of GOME and TOMS total ozone.

Station	Location	Latitude	Longitude	Instrument	Responsible institution
Ny-Alesund	Spitsbergen	79°N	12°E	SAOZ, UV–visible DOAS	NILU
Longyearbyen	Spitsbergen	78°N	16°E	UV–visible DOAS	NILU
Thule	Western Greenland	76°N	69°W	SAOZ	DMI
Scoresbysund	Eastern Greenland	70°N	22°W	SAOZ	CNRS/DMI
Sodankyla	Finland	67°N	27°E	SAOZ	CNRS/FMI
Zhigansk	Eastern Siberia	67°N	123°E	SAOZ	CNRS/CAO
Harestua	Norway	60°N	10°E	UV–visible DOAS	BIRA-IASB
Aberystwyth	United Kingdom	52°N	4°W	SAOZ	U. Wales
Hohenpeissenberg	Germany	48°N	11°E	Dobson, Brewer	Deutsche Wetterdienst
Jungfraujoch	Switzerland	47°N	8°E	SAOZ	BIRA-IASB
Arosa	Switzerland	46°N	9°E	Dobson, Brewer	ETH-Zürich
Bordeaux	France	46°N	1°W	Dobson	U. Bordeaux
Haute Provence	France	44°N	6°E	Dobson, SAOZ	U. Reims, CNRS
Tarawa	Kiribati	1°N	173°E	SAOZ	CNRS/NIWA
Saint-Denis	Reunion Island	21°S	55°E	SAOZ	U. Reunion
Bauru	Brazil	22°S	49°W	SAOZ	CNRS/UNESP
Kerguelen	Kerguelen Islands	49°S	70°E	SAOZ	CNRS
Vernadsky/Faraday	Antarctica	65°S	64°W	Dobson	BAS/KTSU
Dumont d'Urville	Antarctica	66°S	140°E	SAOZ	CNRS
Rothera	Antarctica	68°S	68°W	SAOZ	BAS
Halley	Antarctica	76°S	27°W	Dobson	BAS

persion, and the possible differences of sensitivity of the space-based sensors. The time series are too limited to investigate long-term time-dependent drifts. Figure 1 shows the comparison with seven instruments of the NDSC/Alpine station. Figures 2 and 3 illustrate the difference between space- and ground-based data from the Arctic to the Antarctic, as a function of the satellite SZA, for 15 stations of the SAOZ/UV–visible network. Figure 4 shows the comparison with two Dobson of the NDSC/Antarctic station, in ozone ''hole'' conditions in 1996. The comparison is performed with the direct TOMS and GOME level 2 products, without spatial or temporal interpolation. TOMS overpass data only are available for the present study. GOME ground pixels are selected such as the line of sight of the satellite matches at best the actual location of the correlative ground-based measurements, resulting in several ground pixels a day. Described by Lambert et al. (1998a), this comparison methodology produces a significant reduction in the scatter arising from spatial differences in the air masses sampled by GOME and the ground-based instruments. The comparison with Dobson and Brewer measurements is restricted to direct sun observations, except in Antarctica where zenith-sky data are included for cloudy days, and to data points collocated within 300 km and 3 h between the ground-based measurement and the satellite overpass, except in Antarctica and at Hohenpeissenberg where daily means are used.

a. TOMS: Summary of previous validation

As part of the NASA's Mission to Planet Earth program, long-term daily mapping of the global distribution of atmospheric ozone started with the TOMS on board *Nimbus-7,* TOMS-N7, from October 1978 to May 1993, and continued with a second TOMS on board *Meteor-3,* TOMS-M3, from August 1991 to December 1994. A third and a fourth TOMS were launched in summer 1996 to continue this long-term monitoring: TOMS-EP on 2 July on board NASA's *Earth Probe* platform, and TOMS-AD on 17 August onboard the Japanese *ADEOS* satellite. The TOMS-AD data record ended on 29 June 1997 due to a failure on the *ADEOS* spacecraft. A fifth TOMS flight on board the Russian *Meteor 3M* spacecraft is planned for August 2000. The TOMS observes the solar irradiance and the radiance backscattered from the atmosphere and the earth's surface in the ultraviolet range, in six wavelength bands (Heath et al. 1975; McPeters and Labow 1996). The 1.1-nm bands are centered on 312.5, 317.5, 331.2, 340, 360, and 380 nm for both TOMS-N7 and TOMS-M3, and on 308.6, 312.5, 317.5, 322.3, 331.2, and 360.0 nm for TOMS-AD and TOMS-EP. A mirror scans $\pm 51^\circ$ across track in 35 steps of 3 degrees. With its 800-km polar orbit, TOMS-AD provided a daily global coverage with a ground pixel of 40 km across track $\times$ 40 km along track. To complement the *ADEOS* mission, the 500-km polar orbit of TOMS-EP yields smaller ground pixels and consequently it provides full daily global coverage only beyond 60 degrees of latitude. The TOMS algorithm derives total ozone from radiometric observations by correlating measured radiance with that calculated by a radiative transfer model assuming vertical distributions of ozone density and temperature, after determination of an optimal combination of profiles from a climatological database. The latter is built up from real measurements and is organized into three latitude belts (low, middle, and high latitudes) and by range of ozone column amount.

Total ozone derived from the *Nimbus-7* TOMS radiometric measurements with the successive versions 5 (first publicly available), 6, and 7 (current version) of

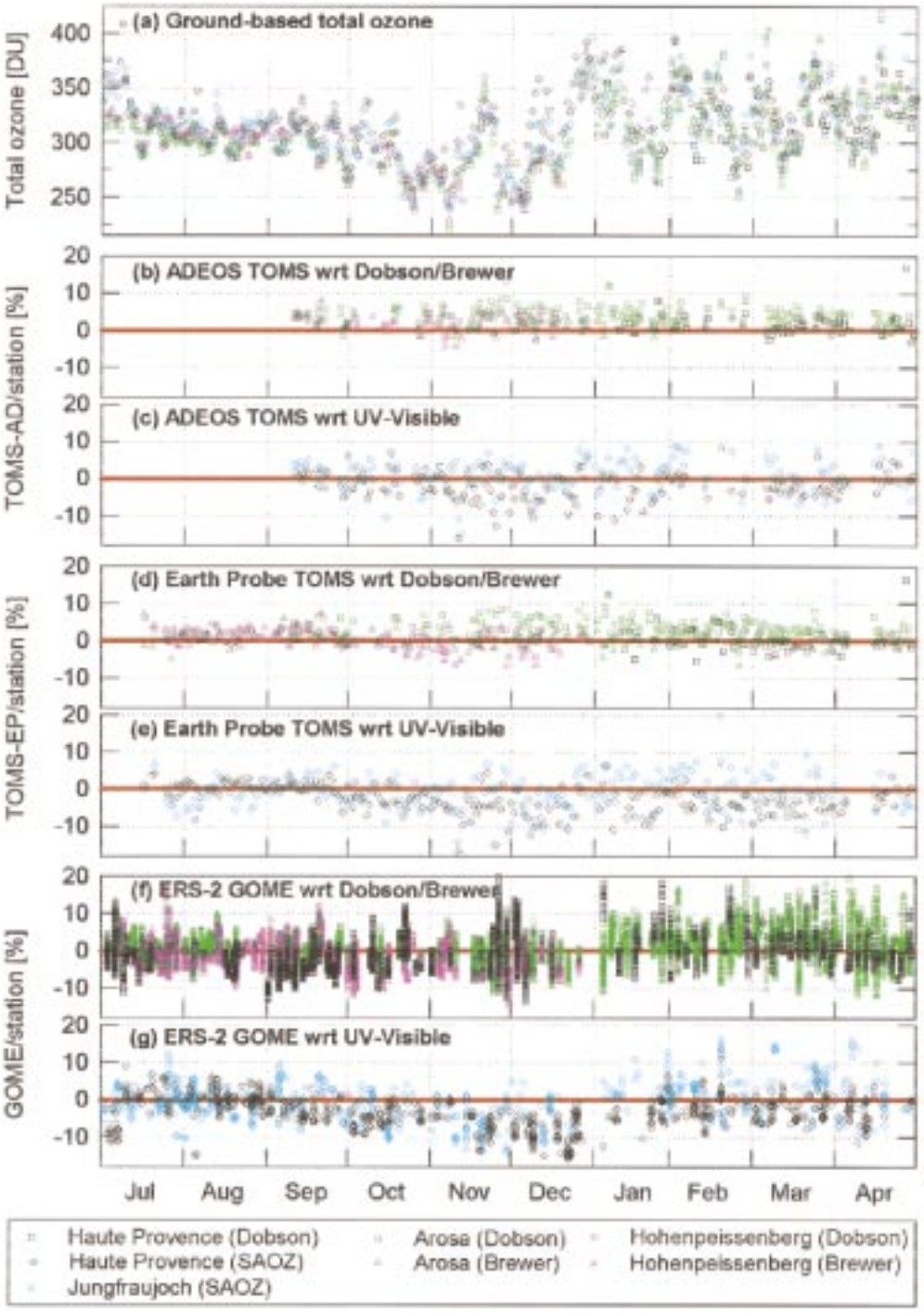

FIG. 1. Comparison between spaceborne and ground-based ozone sensors at the NDSC Alpine station: (a) time series of ground-based total ozone daily means at four different sites in the Alps; (b)–(e) percent relative difference of the *ADEOS* TOMS and of the *Earth Probe* TOMS total ozone with respect to ground-based observations; and (f)–(g) percent relative difference between the GOME and ground-based observations.

the TOMS-N7 data processor has been compared to Dobson measurements at many occasions (e.g., Bhartia et al. 1984; McPeters and Labow 1996). First comparison results between TOMS-N7 V5 and SAOZ total ozone at the polar circles were reported by Pommereau et al. (1989), highlighting a significant SZA dependence. TOMS-N7 V5 was found to produce values much lower than those of SAOZ by 20% at 80° SZA and by 30%

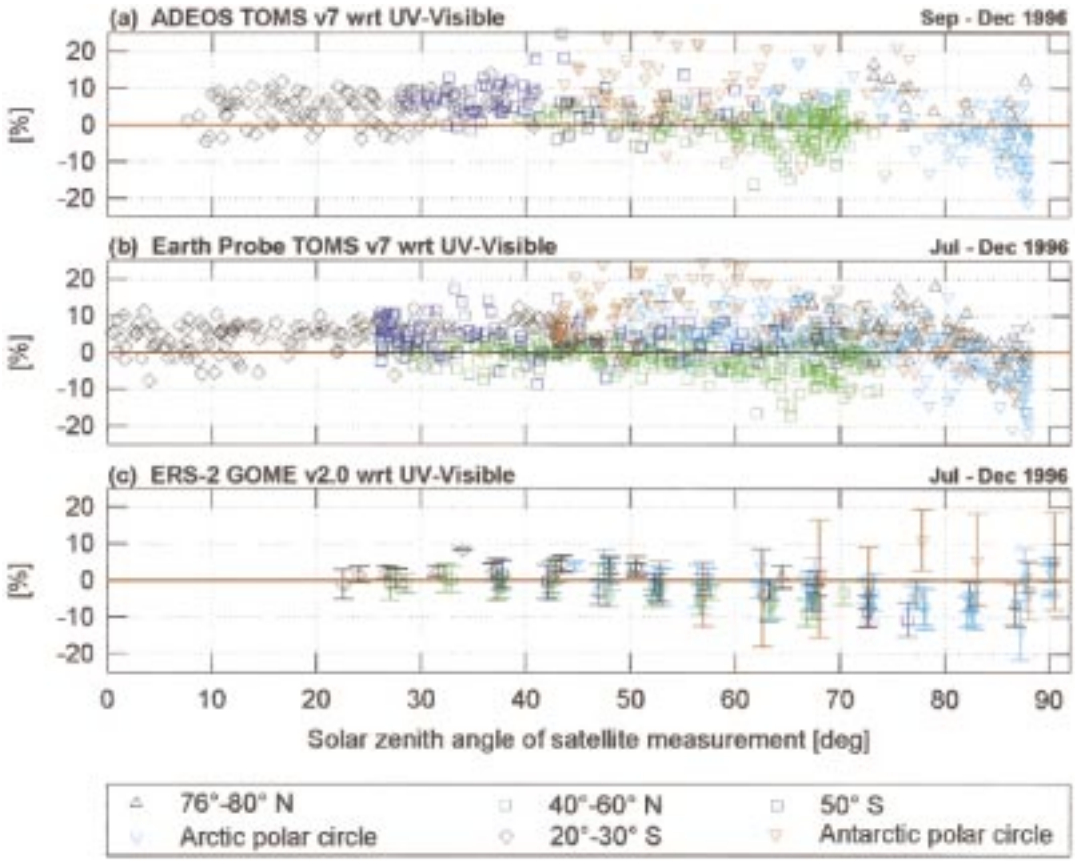

FIG. 2. Solar zenith angle dependence of the consistency between satellite and UV–visible total ozone from pole to pole: percent relative difference of (a) the *ADEOS* TOMS, (b) the *Earth Probe* TOMS, and (c) the GOME total ozone, with respect to ground-based observations from summer through December 1996. Results with GOME are averaged by 5° SZA and vertical bars show the 1 σ confidence level.

beyond 85° SZA. Part of the SZA dependence was identified to originate in the TOMS-N7 algorithm version 5 (Stolarski et al. 1991). Pommereau et al. (1995) and McPeters and Labow (1996) compared versions 6 and 7 of TOMS-N7 total ozone with year-round SAOZ measurements in Antarctica and with 14.5 years of Dobson and Brewer observations at 30 northern stations, respectively. In Antarctica, the comparison demonstrated (i) a significant reduction of the strong SZA dependence observed with V5, (ii) a significant, general improvement between V5 and V6, but (iii) a less clear difference between V6 and V7 and (iv) a seasonal variation of the difference TOMS-N7/SAOZ with both of the latest versions. In the Northern Hemisphere, the study confirmed (i) the significant reduction of the SZA dependence up to 80° SZA and concluded to (ii) an average agreement within ±1%, (iii) an improvement of the time-dependent drift between TOMS-N7 V7 and the ground-based data compared to the drift observed with V6, and (iv) a residual total column dependence of about 1% per 100 DU. Here, we present the first comparison of total ozone derived from the TOMS V7 on board the *ADEOS* and *Earth Probe* satellites, with ground-based data gathered at all latitudes from pole to pole.

b. *Ground-based analysis of the TOMS-AD and TOMS-EP ozone data*

The analysis of the comparison time series demonstrates that the TOMS and the ground-based instruments capture similarly the day-to-day variability of total ozone, in the Alps (Fig. 1) as well as near the edge of the Antarctic polar vortex during springtime ozone depletion (Fig. 4). At northern middle latitudes, the average agreement is better than 2%–3% with both TOMS-AD and TOMS-EP. A similar agreement was observed with the previous TOMS-N7 and TOMS-M3. A seasonal signature appears in the relative differences depicted in Figs. 1b–e. The amplitude of this signature varies with the instrument and the station, and it is likely to arise mainly from the airmass dependence of the direct sun observations and the seasonal variation of the zenith-sky AMF. In particular, it can be seen in Figs. 1c and 1e that the seasonal variation observed in the dif-

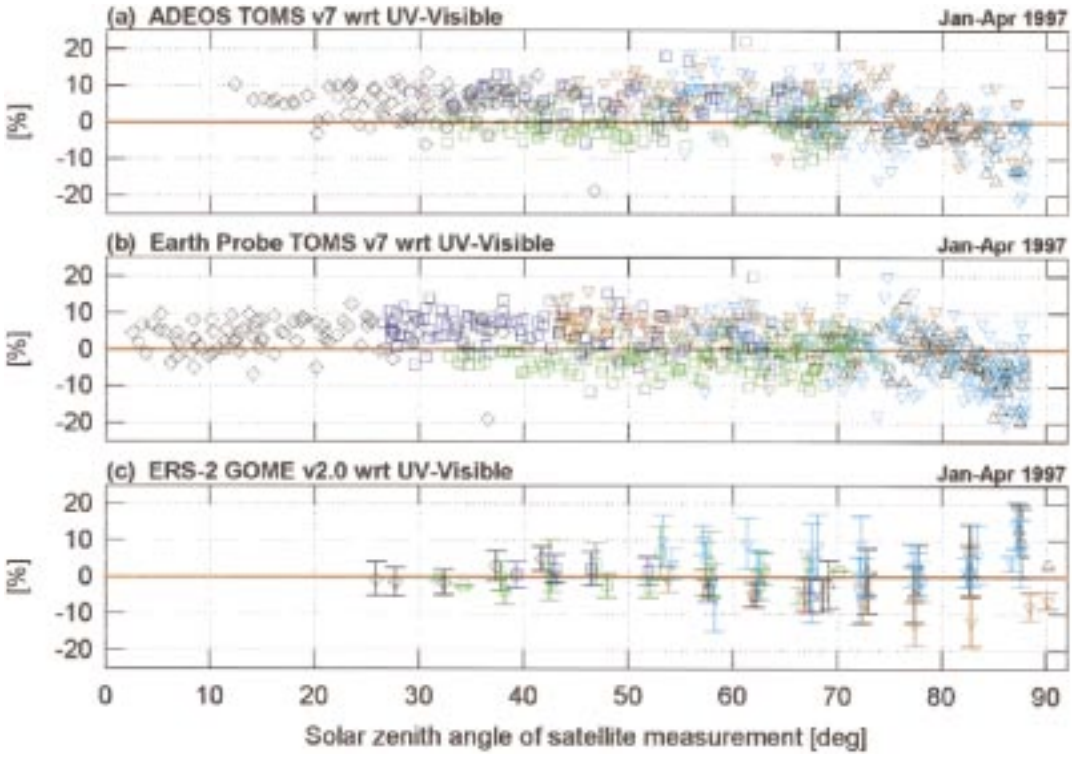

FIG. 3. As in Fig. 2 but from January through April 1997.

ference between TOMS and real-time SAOZ data in Haute Provence is significantly reduced at the Jungfraujoch where SAOZ data are retrieved with seasonal AMFs. The comparison in Fig. 1 also reveals a 2% bias between the results with TOMS-AD and with TOMS-EP, reflecting a bias between TOMS-AD and TOMS-EP data themselves. A similar bias is observed at all latitudes in both hemispheres, its amplitude varying with the latitude. In the Arctic, the signature of a SZA-dependent difference appears that varies slightly with the season. At low and moderate SZA, the TOMS total ozone is larger than that of SAOZ by 3%–5% in summer–fall (Fig. 2), while the agreement is better in wintertime (Fig. 3). Beyond 80° SZA, the ground-based column is larger than that of both TOMS by 5%–10% on average. TOMS/SAOZ differences at Zhigansk are a few percent larger. This latter offset is known to originate partly in the SAOZ real-time data available only at the moment but also partly in the deviation of the actual ozone and temperature profiles over Siberia from those used in the TOMS and SAOZ retrievals. In the Southern Hemisphere, the TOMS are reporting larger columns than the ground-based instruments. At low and middle latitudes, the overestimation is of the order of 5%–8% on average (Figs. 2 and 3). At the three SAOZ and Dobson stations around the Antarctic Circle (Figs. 2–4), the agreement is better in winter likely because of the SZA dependence as observed in the Arctic; however, a systematic bias of 7%–10% appears after September as the SZA decreases. Finally, at the high Antarctic site of Halley, a permanent offset of 8%–12% is observed for the whole winter–spring season. The reported biases in Antarctica do not vanish in summer. It is worth noting that, at all southern latitudes, the total ozone overestimation by TOMS is systematic at low reflectivity, when the measurements are not expected to be disturbed by the cloud cover. At Kerguelen Islands, high reflectivity yields a better agreement. The dataset is still too limited to detect any dependence on the total column, except in the southern Tropics where the average TOMS/SAOZ difference varies from about +6% for total columns lower than 260–270 DU to ±2% at larger values.

When the number of comparison points is large enough to get relevant statistics and after removal of the average difference as a function of time, the scatter between the TOMS and the ground-based total ozone increases, from ±2%–3% (Dobson and Brewer) or from ±4% (SAOZ) at middle latitudes and the Southern Tropics, and up to ±10% at high latitudes and at large SZA. Similar results are obtained with the previous TOMS. As suggested by Lambert et al. (1998a), the lower dispersion with Dobson and Brewer measurements originates mainly in their better spatial and temporal coincidence with the TOMS measurements. The impact of the coincidence of air masses appears clearly in Fig. 1. When the ozone field changes across the Alps rapidly (e.g., on 10 November), the comparison of TOMS total

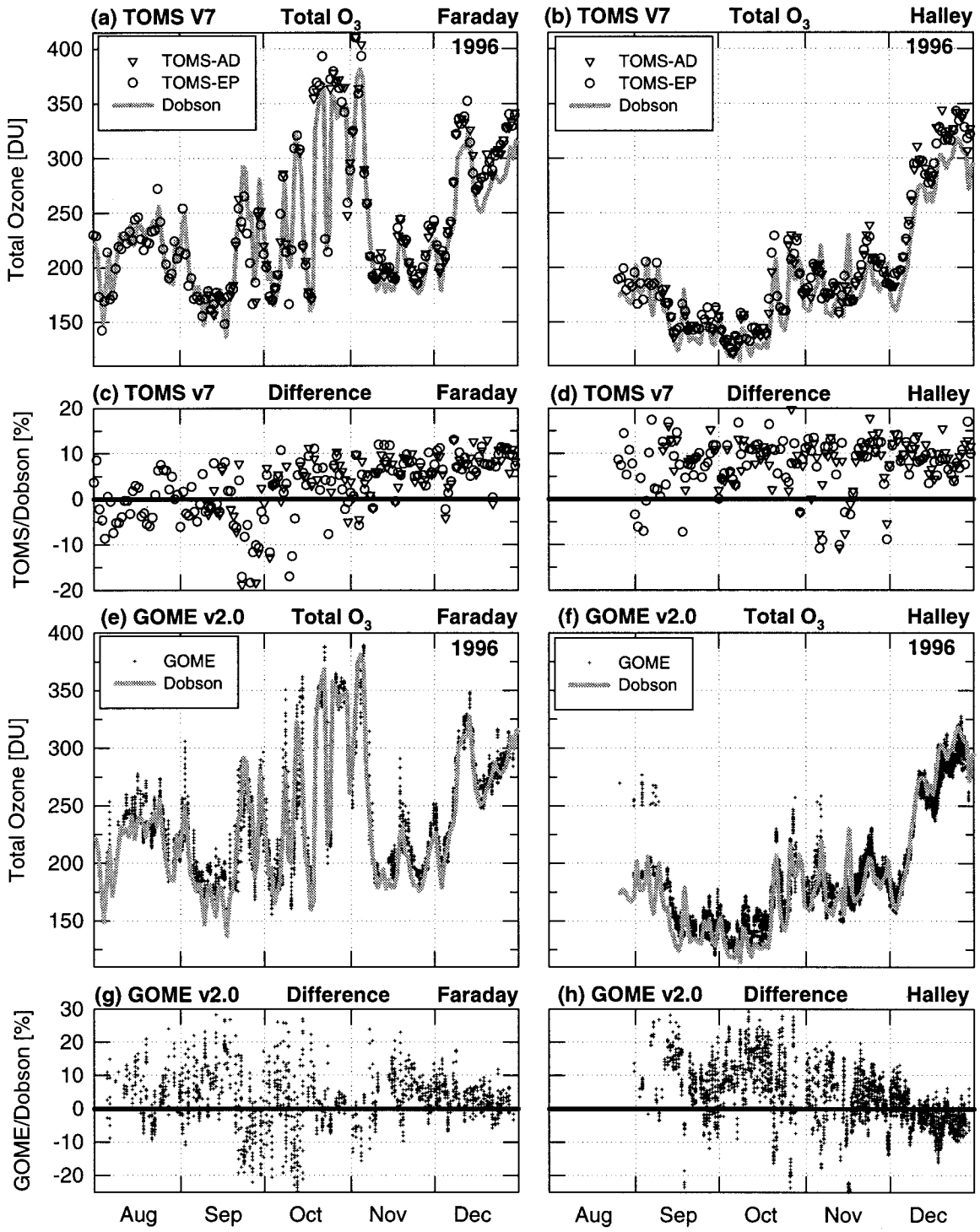

FIG. 4. Comparison between satellite and Dobson observations of total ozone in Antarctica during winter and spring 1996. (a) and (b) Time series of total ozone measured by TOMS-AD, TOMS-EP, and Dobson instruments at Vernadsky/Faraday and at Halley; (c) and (d) corresponding percent relative difference; (e) and (f) total ozone measured by GOME and by Dobson at Vernadsky/Faraday and at Halley; (g) and (h) corresponding percent relative difference.

ozone with individual Dobson and Brewer data can yield significantly much smaller deviations than with individual SAOZ data, although the SAOZ and Dobson daily means depicted in Fig. 1a are in reasonable agreement. The scatter also varies from one station to another, depending on its proximity to local sources of tropospheric ozone and cloudiness. The smallest scatter is observed in the Tropics and at northern midlatitudes in summer, where total stratospheric ozone is very stable in space and in time, and with the near absence of clouds. The dispersion is already larger in northern winter, when the ozone field changes rapidly, and over Brazil during the season when scattered high-altitude clouds are frequent. The largest dispersion between the TOMS and ground-based data—up to 100% in a few extreme cases—is observed at the edge of the polar vortex during springtime ozone depletion. This aberrant dispersion results from large airmass differences and must be discriminated to allow investigations on possible differences in the algorithms or in the measurements. In this work, this discrimination has been based on the analysis of ozone maps from both TOMS and GOME, of the short-term fluctuations observed by the ground-based instruments, and of local meteorological observations.

c. The GOME mission: Previous validation

Launched by ESA on 21 April 1995 on board its *ERS-2* environmental satellite, the GOME (Burrows et al. 1999) consists of a nadir-viewing UV–visible grating spectrometer observing, between 240 and 790 nm, the solar irradiance and the solar radiation backscattered from both the atmosphere and the earth's surface. A mirror scans across track three ground pixels of 320 km across track $\times$ 40 km along track. The 960 km $\times$ 40 km backscan pixel is recorded as well. Atmospheric abundances of ozone and NO_2, as well as other relevant trace species, such as BrO, OClO, SO_2, and CH_2O, are inferred from GOME spectral observations by the application of the DOAS technique to the ratio between the earth's radiance and solar irradiance. In particular, apparent slant column amounts of ozone and NO_2 are routinely retrieved in the 325–335-nm and 425–450-nm spectral windows, respectively. Slant column amounts are converted into vertical column amounts by means of modeled AMFs. AMFs down to the top of clouds and down to the ground are calculated by a multiple-scattering, radiative transfer model. Information on cloud cover and cloud-top height is derived from GOME measurements around the O_2 A band at 760 nm. The AMF calculation uses vertical distributions of absorbing species, pressure, and temperature, which are derived from 2D chemical-transport model results and sorted by season and into 18 latitude belts from north to south.

Ground-based instruments in general, the NDSC and the SAOZ/UV-visible network in particular, have played a major role during the maturity of the *ERS-2* GOME Data Processor's developmental version (GDP version 1.x) and of its first publicly available version (GDP 2.0). Based on 45 days of data from July to December 1995, a first analysis of the GOME total ozone retrieved with GDP 1.20–1.21 was conducted, among others, with various ground-based observations from the NDSC Alpine station (Lambert et al. 1996a), from the Norwegian monitoring network (Hansen and Dahlback 1996), and from the pole-to-pole SAOZ/UV–visible network (Lambert et al. 1996b). Those exercises concluded to (i) a general underestimation of total ozone by the GOME; (ii) a significant SZA dependence at all latitudes: 5% average underestimation at 45° SZA, 10% at 60° SZA, and irrelevant data beyond 75° SZA; (iii) a difference of sensitivity to total ozone between the GOME and the SAOZ instruments; and (iv) an overestimation of the ozone column by 10%–20% at high latitudes in summer, as well as during springtime ozone hole conditions over Antarctica. Following the recommendations and conclusions drawn from this first exercise, the GOME ozone retrieval in the Huggins band has been revisited and improvements have led to the current GDP version 2.0. A preliminary comparison between the GOME V2.0 and ground-based total ozone in July–August 1996 was conducted at northern latitudes by Van Roozendael et al. (1998b) and from pole to pole by Lambert et al. (1998b), by means of observations from Dobson, Brewer, SAOZ, and UV filter radiometers. As a result, a generally better agreement between the satellite and the ground-based measurements was demonstrated, although a persistent SZA dependence remained. Here, a nearly year-round ground-based analysis of the GOME V2.0 total ozone is reported. The study is based on comparisons with UV–visible observations from pole to pole, and with Dobson and Brewer observations in the Alps and in Antarctica, over the period from 28 June 1996 through 30 April 1997.

d. Ground-based analysis of the ERS-2 *GOME total ozone*

From pole to pole, the comparison shows that the GOME and the ground-based instruments are all capturing the high day-to-day variability similarly, as illustrated in Fig. 1 for the NDSC/Alpine station and in Fig. 4 for ozone hole conditions in Antarctica. At northern middle latitudes up to 60°N, the average agreement between the GOME and ground-based total ozone is better than $\pm 4\%$. At the Jungfraujoch, where the retrieval algorithm takes into account the 3% seasonal cycle of the SAOZ AMF and the altitude of the station (3580 m MSL), the GOME and SAOZ observations are consistent, on average, to within 2%, that is, within the uncertainty of the SAOZ measurement. Figures 1f and 1g reveal a small shift in the Alps between GOME data from December 1996 and from January 1997. A consistency to within 2%–4% is also observed at the southern middle latitudes and Tropics. In the Arctic, the average agreement between GOME and SAOZ depends

TABLE 2. Summary of the consistency between space-based (TOMS-AD, TOMS-EP, and *ERS-2* GOME) and ground-based total ozone.

	TOMS	GOME
Northern midlatitudes	Good agreement, better than ±2%–3%	Good agreement, better than ±2%–4%
Arctic	Good agreement at moderate SZA: ±4% SZA dependence beyond 80°SZA	Good agreement at moderate SZA: ±4% SZA dependence beyond 70° SZA
Southern Hemisphere	Systematic overestimation of about 5%–10% at all latitudes	Good general agreement in ''normal'' conditons: ±2%–4%.
SZA dependence	5%–10% underestimation beyond 80% SZA	Summer–fall: 5%–10% underestimation between 70° and 85° SZA Winter–spring: 10% overestimation beyond 85° SZA
	Small seasonal variation	Small latitudinal variation
Difference in sensitivity	Overestimation of low ozone at the southern Tropics	High latitudes and southern Tropics: –overestimation of low ozone –relative differences correlate with the ozone column values
Internal bias	Small bias between TOMS-AD and TOMS-EP total ozone	Small shift in the Alps between data from December 1996 and from January 1997

clearly on the SZA of the GOME observation and on the season. Below 70° SZA, the mean difference does not exceed ±4%, except at Zhigansk for the same reasons as aforementioned. Between 70° and 85° SZA, the mean difference remains lower than ±4% in winter–spring (Fig. 3), but in summer–fall it decreases down to 5%–10%, with a minimum at 75°–80° SZA (Fig. 2). Beyond 85° SZA, the GOME total ozone values increase compared to those measured between 70° and 85° SZA, resulting in positive mean differences of about 10% in winter–spring, but a reasonable agreement in summer–fall. The particular shape and the seasonal variation of the GOME SZA dependence are similar at both polar circles, however slightly more pronounced in Antarctica. It appears clearly in Figs. 4g and 4h that the difference between the GOME and Dobson data correlates with the total ozone under Antarctic ozone hole conditions. While the agreement is reasonable around 300 DU, GOME is overestimating systematically the lowest columns and underestimating the highest ones. A similar difference in sensitivity is observed around both the Antarctic and Arctic Circles, and around the southern Tropics where GOME overestimates low SAOZ total ozone values (<260 DU) and underestimates higher values, by about 4% on average. At the high Antarctic station of Halley, the GOME total ozone measured from August through October is overestimated by 11% on average compared to Dobson (Fig. 4h). The difference in sensitivity can explain this bias as partly due to the permanent very low total ozone values ranging from 100 DU up to a maximum of 210 DU at this station. It explains also why the bias vanishes in December as the total ozone recovers to normal values.

After removal of the average difference as a function of time, the scatter between GOME and ground-based total ozone at the southern Tropics and at middle latitudes ranges from ±2% to ±4%, the scatter with SAOZ being slightly larger than that observed when compared with the Dobson and Brewer. It can increase up to ±10% at high latitudes and for SZA larger than 70°. The analysis of the dispersion with respect to the season, the SZA, and other parameters yields similar conclusions to those drawn from the analysis of the TOMS data.

e. Discussion and conclusions

The key results of the comparisons between space- and ground-based total ozone are listed in Table 2. TOMS-AD, TOMS-EP, and GOME data are found to be globally consistent with ground-based observations. However, the comparisons reveal several discrepancies. Some of them are common but not always similar among the two types of spaceborne sensors: the SZA dependence at high latitudes, the discrepancies over Antarctica in springtime, and the systematic bias between satellite and SAOZ observations of low ozone columns at the southern Tropics. Although exhibiting systematic differences, the results obtained with TOMS-AD and with TOMS-EP are consistent within a few percent, but these also show a systematic interhemispheric difference with the ground-based observations. The results obtained with GOME do not reveal any significant interhemispheric feature, but a difference in sensitivity between the GOME and ground-based sensors at high latitudes.

Except at the Jungfraujoch, Harestua, and Spitsbergen stations, the preliminary ground-based datasets are not corrected for the seasonal/latitudinal variation of the zenith-sky AMF, nor for the temperature and airmass dependences of the Dobson and Brewer measurements, which could contribute partly to the SZA dependence. However, they certainly cannot account for the full systematic bias observed at high SZA, nor for the shape of the SZA dependence, which, in addition, is different for GOME and for TOMS. The SZA dependence can be observed at high latitudes in the satellite data them-

selves since in polar areas in summertime this dependence generates a systematic bias between satellite data of the descending and ascending orbits, around noon and midnight sun. Ultraviolet radiance measurements at nadir are known to be sensitive to the shape of the ozone, pressure, and temperature profiles. The difference between the GOME and the TOMS comparisons might arise from basic algorithm differences in the treatment of the profile shape effect. Indeed, in the one-step treatment included in the GOME V2.0, the profile is specified for a given latitude belt during a given season, while in the iterative approach of TOMS V7, the shape of the profile is optimized according to the latitude and the amplitude of the ozone column. The seasonal/latitudinal variation of the GOME SZA dependence might vindicate the use of a climatology based on real profile measurements, such as the TOMS V7 climatology. An overcorrection for multiple scattering, different for the GOME and TOMS algorithms, cannot be ruled out. The profile shape effect can also account partly for the correlation observed at high latitudes between the ozone column value and the difference of GOME with ground-based data. This difference in sensitivity might be related to the use of monthly atmospheric profiles in the GOME retrieval that cannot match the actual, highly variable atmospheric profile. The effect would be significantly reduced with TOMS since it uses a column-resolved climatology. In addition, at higher SZA, the TOMS algorithm uses measurements at the shorter wavelengths to optimize the combination of mid- and high-latitude profiles. Since the apparent slant column amount of absorber increases with SZA, both the difference in sensitivity and the particular shape of the GOME SZA dependence might also result from the particular approach of DOAS adopted in GDP 2.0, and especially from (i) the use of a single wavelength for the calculation of the GOME AMF, although this latter varies significantly over the fitting spectral window; (ii) a small wavelength registration shift between the GOME spectra and the laboratory cross sections; (iii) the incorrect removal of the Fraunhofer solar lines; and (iv) an imperfect convolution of ozone cross sections. Overall, the results shown are still too scarce to demonstrate a difference of sensitivity between the TOMS and ground-based instruments. An exception is the southern Tropics where the three satellite instruments measure systematically higher values at low ozone. It remains to be seen if this could be explained by a combination of low signal-to-noise at low SZA, and profile shape effect in the spaceborne sensors, or by a systematic bias of the zenith-sky AMFs. The pole-to-pole comparison points out a clear north–south difference in the agreement between TOMS and ground-based data. In particular, the TOMS overestimate the ground-based columns in Antarctica by 8%–12%, while the agreement is reasonable in the Arctic. This interhemispheric difference might arise from the climatology of ozone and temperature profiles used in the TOMS V7 algorithm. These profiles are derived from a composite climatology of SAGE II and ozonesonde datasets. The TOMS V7 climatology is hence somewhat biased toward the Northern Hemisphere. In addition, higher altitudes are poorly represented at polar latitudes since there are very few SAGE II measurements beyond the polar circle. The interhemispheric consistency of GOME seems to vindicate a separate treatment of each hemisphere. At Antarctic stations, both the cloud cover fraction (GOME) and the reflectivity (TOMS) demonstrate an almost permanent overcast. The tropospheric contribution to the satellite measurement is partly masked and a climatological ozone profile below clouds must be used, which can also introduce an offset in the satellite data. Small errors of the TOMS calibration in the Southern Hemisphere cannot be excluded. Calibration uncertainties might partly explain the difference between TOMS-AD and TOMS-EP data as well.

After removal of the average difference as a function of time, the dispersion of satellite data with respect to ground-based observations is similar for GOME and TOMS. It increases from $\pm 2\%$–3% in the Tropics and at middle latitudes, up to $\pm 10\%$ at high latitudes in winter and also at high SZA. A first contribution to this scatter is related to the spatial and temporal difference in air masses probed by the spaceborne and the ground-based instruments, combined with the presence of horizontal gradients and of variability (Lambert et al. 1998a). The scatter is smaller with Dobson and Brewer measurements performed within about three hours around the GOME and TOMS overpasses. It increases with UV–visible zenith-sky observations at twilight, partly due to the difference of measurement time and the large horizontal extension of the zenith-sky air mass (about 350 km toward the sun at twilight) compared to the direct sun air mass. At low sun elevation, a lower scatter might be expected between nadir-viewing spaceborne and zenith-sky ground-based observations, since both measure, within a few hours, coincident air masses extending over several hundred kilometers in the same direction. However, the opposite is observed, partly due to the low sensitivity of UV nadir measurements at high SZA to the lower atmosphere and partly due to the uncertainty on radiative transfer modeling in the ultraviolet when SZA increases. Another important source of scatter originates in deviations of the actual ozone, pressure, and temperature profiles from those in use in the retrievals. Other possible contributions are related to the cloud cover: (a) perturbations generated in the ground-based measurements (mainly the SAOZ) by tropospheric multiple scattering in presence of dense clouds or haze, combined with local ozone changes; (b) uncertainties in the cloud treatment in the satellite retrieval (e.g., uncertainties in optical properties of clouds or the use of a climatological database for cloud-top pressure); (c) perturbations due to dense (type II) polar stratospheric clouds in winter polar regions; and (d)

clouds that mask the tropospheric contribution of the satellite measurements.

To conclude, the global picture of total ozone provided from summer 1996 through April 1997 by the three space-based sensors studied in this work is globally consistent with high quality ground-based observations associated with the NDSC. Nevertheless, further investigation is required to understand the various discrepancies identified in this preliminary study. Several issues should be addressed, such as the hemispheric separation of the TOMS V7 climatology; possible calibration problems with TOMS, especially in the Southern Hemisphere; an iterative treatment of the profile shape effect with the GOME, using a column-resolved climatology based on real profile measurements; and refinements of the current DOAS approach used in GOME.

Acknowledgments. For providing high quality data in near–real time and for fruitful discussions, the authors address all their acknowledgments to the contributing instrument PIs and operators, and especially to S. B. Andersen and P. Eriksen (DMI), D. W. Arlander, K. Karlsen Tørnkvist, B. A. Kåstad Høiskar, and C. W. Tellefsen (NILU), A. Barbe and M.-F. Merienne (University Reims), N. A. Bui Van (UNESP), H. Claude (Deutsche Wetterdienst), J. de La Noë (University of Bordeaux), V. Dorokhov (CAO), E. Kyrö (FMI), J. Leveau (University of Réunion), G. Milinevsky (KTSU), H. K. Roscoe and J. D. Shanklin (BAS), J. Staehelin (ETH-Zürich), G. Vaughan (University of Wales), and R. Zander (University of Liège). They greatly appreciate the computational and logistic support provided by P. Gerard and J. Granville from IASB and J. Hottier from CNRS. TOMS V7 overpass data and GOME V2.0 level 2 products were processed at the NASA/Goddard Space Flight Center and at the German Remote Sensing Data Centre (DFD/DLR), respectively. This work has been supported by the PRODEX-GOME A.O. *ERS-2* Project 1 and by the Belgian State–Prime Minister's Service, Science Policy Office (Contract GC/35/002) in Belgium, by the Programme National de Chimie de l'Atmosphère in France, and by the European Commission (DG XII) in the frame of the ESMOS and SCUVS projects, Contracts EV5V-CT93-0348, EV5V-CT95-0084 and EV5V-CT93-0334.

REFERENCES

Abbas, M. M., T. Kostiuk, M. J. Mumma, D. Buhl, V. G. Kunde, and L. W. Brown, 1978: Stratospheric ozone measurement with an infrared heterodyne spectrometer. *Geophys. Res. Lett.,* **5,** 317–320.

Basher, R. E., 1994: Survey of WMO-sponsored Dobson spectrophotometer intercomparisons. WMO Global Ozone Research and Monitoring Project Rep. No. 19, WMO, Geneva, Switzerland, 54 pp.

Bhartia, P. K., K. F. Klenk, C. K. Wong, and D. Gordon, 1984: Intercomparison of the Nimbus 7 SBUV/TOMS total ozone data sets with Dobson and M83 results. *J. Geophys. Res.,* **89,** 5239–5247.

——, J. Herman, and R. D. McPeters, 1993: Effect of Mount Pinatubo aerosols on total ozone measurements from backscatter ultraviolet (BUV) experiments. *J. Geophys. Res.,* **98,** 18 547–18 554.

Brewer, A. W., C. T. McElroy, and J. B. Kerr, 1973: Nitrogen dioxide concentrations in the atmosphere. *Nature,* **246,** 129–133.

Brion, J., A. Chakir, D. Daumont, J. Malicet, and C. Parisse, 1993: High resolution laboratory cross-sections of O_3, temperature effect. *Chem. Phys. Lett.,* **6,** 612.

Burkholder, J. B., and R. K. Talukdar, 1994: Temperature dependence of the ozone absorption spectrum over the wavelength range 410 to 760 nm. *Geophys. Res. Lett.,* **21,** 581–584.

Burrows, J. P., M. Weber, M. Buchwitz, 1999: V. Rozanov, A. Ladstaetter-Weissenmayer, A. Richter, R. De Beek, R. Hoogen, K. Bramstedt, K.-U. Eichmann, and M. Eisinger. The Global Ozone Monitoring Experiment (GOME): Mission concept and first scientific results. *J. Atmos. Sci.,* **56,** 151–175.

Coquart, B., A. Jenouvrier, and M.-F. Merienne, 1995: The NO_2 absorption spectrum II. Absorption cross sections at low temperature in the 400–500 nm region. *J. Atmos. Chem.,* **21,** 251–261.

Cunnold, D. M., J. M. Zawodny, W. P. Chu, J. P. Pommereau, F, Goutail, J. Lenoble, M. P. McCormick, R. E. Veiga, D. Murcray, N. Iwagami, K. Shibasaki, P. C. Simon, and W. Peetermans, 1991: Validation of SAGE II NO_2 measurements. *J. Geophys. Res.,* **96,** 12 913–12 925.

Dahlback, A., 1995: The influence of clouds on Dobson measurements. *Proc. Third European Symp. on Polar Stratospheric Ozone,* Schliersee, Bavaria, Germany, European Commission, 527–531.

——, 1996: Measurements of biologically effective UV doses, total ozone abundances, and cloud effects with multichannel, moderate bandwidth filter instruments. *Appl. Opt.,* **35,** 6514–6521.

De Backer, H., and D. De Muer, 1991: Intercomparison of total ozone data measured with Dobson and Brewer ozone spectrophotometers at Uccle (Belgium) from January 1984 to March 1991, including zenith sky observations. *J. Geophys. Res.,* **96,** 20 711–20 719.

De Mazière, and Coauthers, 1998a: Towards improved evaluations of total ozone at the Jungfraujoch, using vertical profile estimations based on auxiliary data. *Atmospheric Ozone—Proceedings of the 18th Quadrennial Ozone Symposium,* R. D. Bojkov and G. Visconti, Eds., Vol. I, 25–28.

——, M. Van Roozendael, C. Hermans, P. C. Simon, P. Demoulin, G. Roland, and R. Zander, 1998b: Quantitative evaluation of the post-Pinatubo NO_2 reduction and recovery, based on 10 years of Fourier transform infrared and UV-visible spectroscopic measurements at Jungfraujoch. *J. Geophys. Res.,* **103,** 10 849–10 858.

De Muer, D., and H. De Backer, 1992: Revision of 20 years of Dobson total ozone data at Uccle (Belgium): Fictitious Dobson total ozone trends induced by sulfur dioxide trends. *J. Geophys. Res.,* **97,** 5921–5937.

Denis, L., and Coauthors, 1995: SAOZ total O_3 and NO_2 at the southern tropics and equator. *Proc. Third European Symp. on Polar Stratospheric Ozone,* Schliersee, Bavaria, Germany, European Commission, 458–462.

Dobson, G. M. B., 1957: Observer's handbook for the ozone spectrophotometer. *Annales International Geophysical Year, V, Part I: Ozone,* Pergamon, 46–89.

Gordley, L. L., J. M. Russell, L. J. Mickley, J. E. Frederick, J. H. Park, K. A. Stone, G. M. Beaver, J. M. McInerney, L. E. Deaver, G. C. Toon, F. J. Murcray, R. D. Blatherwick, M. R. Gunson, J. P. D. Abbatt, R. L. Mauldin, G. H. Mount, B. Sen, and J.-F. Blavier, 1996: Validation of nitric oxide and nitrogen dioxide measurements made by the Halogen Occultation Experiment for UARS platform. *J. Geophys. Res.,* **101,** 10 241–10 266.

Götz, F. W. P., A. A. Meethan, and G. M. B. Dobson, 1934: The vertical distribution of ozone in the atmosphere. *Proc. Roy. Soc. London,* **145A,** 416–446.

Hansen, G., and A. Dahlback, 1996: Validation of total ozone measurements with GOME during the main validation phase: The Norwegian project. *Proc. GOME Geophysical Validation Final Results Workshop,* Frascati, Italy, ESRIN, ESA, 199–208.

Harwood, M. H., and R. L. Jones, 1994: Temperature dependent ultraviolet cross-sections of NO_2 and N_2O_4: Low temperature measurements of the equilibrium constant $2NO_2 \leftrightarrow N_2O_4$. *J. Geophys. Res.,* **99,** 22 955–22 964.

Heath, D. F., A. J. Krueger, H. A. Roeder, and B. D. Henderson, 1975: The solar backscatter ultraviolet and total ozone mapping spectrometer (SBUV/TOMS) for NIMBUS G. *Opt. Eng.,* **14,** 323–331.

Hegels, E., and D. Perner, 1996: Validation of GOME BrO Measurements on Sondre Stromfjord, Greenland, *Proc. GOME Geophysical Validation Final Results Workshop,* Frascati, Italy, ESRIN, ESA, 109–113.

Hervig, M. E., J. M. Russell, L. L. Gordley, S. R. Drayson, K. Stone, R. E. Thompson, M. E. Gelman, I. S. McDermid, A. Hauchecorne, P. Keckhut, T. J. McGee, U. N. Singh, and M. R. Gross, 1996: Validation of temperature measurements from the Halogen Occultation Experiment. *J. Geophys. Res.,* **101,** 10 277–10 285.

Hofmann, D., P. Bonasoni, M. De Mazière, F. Evangelisti, A. Sarkissian, G. Giovanelli, A. Goldman, F. Goutail, J. Harder, R. Jakoubek, P. Johnston, J. Kerr, T. McElroy, R. McKenzie, G. Mount, J.-P. Pommereau, P. Simon, S. Solomon, J. Stutz, A. Thomas, M. Van Roozendael, and E. Wu, 1995: Intercomparison of UV/visible spectrometers for measurements of stratospheric NO_2 for the Network for the Detection of Stratospheric Change. *J. Geophys. Res.,* **100,** 16 765–16 791.

Høiskar, B. A. K., A. Dahlback, G. Vaughan, G. O. Braathen, F. Goutail, J.-P. Pommereau, and R. Kivi, 1997: Interpretation of ozone measurements by ground-based visible spectroscopy—A study of the seasonal dependence of air mass factors for ozone based on climatology data. *J. Quant. Spectrosc. Radiat. Transfer,* **57,** 569–579.

Josefsson, W. A. P., 1992: Focused sun observations using a Brewer ozone spectrophotometer. *J. Geophys. Res.,* **97,** 15 813–15 817.

Keckhut, P., M. E. Gelman, J. D. Wild, F. Tissot, A. J. Miller, A. Hauchecorne, M.-L. Chanin, E. F. Fishbein, J. Gille, J. M. Russell III, and F. W. Taylor, 1996: Semidiurnal and diurnal temperature tides (30–55 km): Climatology and effect on UARS-LIDAR data comparisons. *J. Geophys. Res.,* **101,** 10 299–10 310.

Kerr, J. B., C. T. McElroy, and W. F. J. Evans, 1983: The automated Brewer spectrophotometer for measurement of SO_2, O_3 and aerosols. Preprints, *Fifth Symp. Meteorological Observations and Instrumentation,* Toronto, ON, Canada, Amer. Meteor. Soc., 470–472.

——, I. A. Asbridge, and W. F. J. Evans, 1988: Intercomparison of total ozone measured by the Brewer and Dobson spectrophotometers at Toronto. *J. Geophys. Res.,* **93,** 11 129–11 140.

Komhyr, W. D., C. L. Mateer, and R. D. Hudson, 1993: Effective Bass-Paur 1985 ozone absorption coefficients for use with Dobson ozone spectrophotometers. *J. Geophys. Res.,* **98,** 20 451–20 465.

Lambert, J.-C., and Coauthors, 1996a: GOME ozone total amounts validation by ground-based observations performed at the NDSC/Alpine Stations. *Proc. GOME Geophysical Validation Final Results Workshop,* Frascati, Italy, ESRIN, ESA, 115–121.

——, and Coauthors, 1996b: Validation of the ERS-2 GOME products with the SAOZ network. *Proc. GOME Geophysical Validation Final Results Workshop,* Frascati, Italy, ESRIN, ESA, 123–131.

——, ——, J. Granville, P. Gerard, P. C. Simon, H. Claude, and J. Staehelin, 1998a: Comparison of the GOME ozone and NO_2 total amounts at mid-latitude with ground-based zenith-sky measurements. *Atmospheric Ozone—Proceedings of the 18th Quadrennial Ozone Symposium,* R. D. Bojkov and G. Visconti, Eds., Vol. I, 301–304.

——, and Coauthors, 1998b: Validation of the ERS-2 GOME total ozone measurements with the SAOZ ground-based network during the period: 28 June–17 August 1996. *Atmospheric Ozone—Proceedings of the 18th Quadrennial Ozone Symposium,* R. D. Bojkov and G. Visconti, Eds., Vol. I, 297–300.

Liu, X., F. J. Murcray, D. G. Murcray, and J. M. Russel III, 1996: Comparison of HF and HCl vertical profiles from ground-based high-resolution infrared solar spectra with Halogen Occultation Experiment observations. *J. Geophys. Res.,* **101,** 10 175–10 181.

McKenzie, R. L., P. V. Johnston, C. T. McElroy, J. B. Kerr, and S. Solomon, 1991: Altitude distribution of stratospheric constituents from ground-based measurements at twilight. *J. Geophys. Res.,* **96,** 15 499–15 511.

——, ——, M. Kotkamp, A. Bittar, and J. D. Hamlin, 1992: Solar ultraviolet spectroradiometry in New Zealand: Instrumentation and sample results from 1990. *Appl. Opt.,* **31,** 6501–6509.

McPeters, R. D., and G. Labow, 1996: An assessment of the accuracy of 14.5 years of Nimbus 7 TOMS ozone data by comparison with the Dobson network. *Geophys. Res. Lett.,* **23,** 3695–3698.

Menzies, R. T., and M. T. Chahine, 1974: Remote atmospheric sensing with an airborne laser absorption spectrometer. *Appl. Opt.,* **13,** 2840–2849.

Merienne, M. F., A. Jenouvrier, and B. Coquart, 1995: The NO_2 absorption spectrum I: Absorption cross-sections at ambient temperature in the 300–500 nm region. *J. Atmos. Chem.,* **20,** 281–297.

Murata, I., Y. Kondo, H. Nakajima, M. Koike, Y. Zhao, W. A. Matthews, and K. Suzuki, 1997: Accuracy of total ozone column amounts observed with solar infrared spectroscopy. *Geophys. Res. Lett.,* **24,** 77–80.

Nichol, S. E., and C. Valenti, 1993: Intercomparison of total ozone measured at low sun angles by the Brewer and Dobson spectrophotometers at Scott Base, Antarctica. *Geophys. Res. Lett.,* **20,** 2051–2054.

Notholt, J., R. Neuber, O. Schrems, and T. v. Clarmann, 1993: Stratospheric trace gas concentrations in the Arctic polar night derived by FTIR-spectroscopy with the moon as IR light source. *Geophys. Res. Lett.,* **20,** 2059–2062.

Noxon, J. F., E. C. Whipple, and R. S. Hyde, 1979: Stratospheric NO2 1. Observational method and behavior at mid-latitude. *J. Geophys. Res.,* **84,** 5047–5065.

Pommereau, J.-P., and F. Goutail, 1988: Ground-based measurements by visible spectrometry during Arctic winter and spring 1988. *Geophys. Res. Lett.,* **15,** 891–894.

——, ——, H. Le Texier, and T. S. Jorgensen, 1989: Stratospheric ozone and nitrogen dioxide monitoring at southern and northern polar latitudes. *Proc. 28th Liège Int. Astrophysical Colloquium "Our Changing Atmosphere,"* P. J. Crutzen, J.-C. Gerard, and R. Zander, Eds., 141–147.

——, ——, and A. Sarkissian, 1995: SAOZ total ozone measurements in Antarctica. Comparisons with TOMS versions 6 and 7. *Proc. Third European Symp. on Polar Stratospheric Ozone,* Schliersee, Bavaria, Germany, European Commission, 516–520.

Pougatchev, N. S., B. J. Connor, and C. P. Rinsland, 1995: Infrared measurements of the ozone vertical distribution over Kitt Peak. *J. Geophys. Res.,* **100,** 16 689–16 697.

Preston, K. E., R. L. Jones, and H. K. Roscoe, 1997: The retrieval of NO_2 vertical profiles from ground-based UV-visible measurements: Method and validation. *J. Geophys. Res.,* **102,** 19 089–19 097.

——, D. J. Fish, H. K. Roscoe, and R. L. Jones, 1998: Accurate derivation of total and stratospheric vertical columns of NO_2 from ground-based zenith-sky measurements. *J. Atmos. Chem.,* **30,** 163–172.

Ricaud, P., J. de La Noë, B. J. Connor, L. Froidevaux, J. W. Waters, R. S. Harwood, I. A. MacKenzie, and G. E. Peckham, 1996: Diurnal variability of mesospheric ozone as measured by the UARS microwave limb sounder instrument: Theoretical and ground-based validations. *J. Geophys. Res.,* **101,** 10 077–10 089.

Roscoe, H. K., and Coauthors, 1998:Slant column measurements of O_3 and NO_2 during the NDSC intercomparison of zenith-sky UV-visible spectrometers in June 1996. *J. Atmos. Chem.,* in press.

Rothman, L. S., R. R. Gamache, R. H. Tipping, C. P. Rinsland, M. A. H. Smith, D. C. Benner, V. Malathy Devi J.-M. Flaud, C. Camy-Peyret, A. Perrin, A. Goldman, S. T. Massie, L. R. Brown, and R. A. Toth, 1992: The HITRAN molecular database: Editions of 1991 and 1992. *J. Quant. Spectrosc. Radiat. Transfer,* **48,** 469–507.

Russell, J. M., III, L. E. Deaver, M. Luo, J. H. Park, L. L. Gordley, A. F. Tuck, G. C. Toon, M. R. Gunson, W. A. Traub, D. G. Johnson, K. W. Jucks, D. G. Murcray, R. Zander, I. G. Nolt, and C. R. Webster, 1996a: Validation of hydrogen chloride measurements made by the Halogen Occultation Experiment from the UARS platform. *J. Geophys. Res.,* **101,** 10 151–10 162.

——, ——, ——, R. J. Cicerone, J. H. Park, L. L. Gordley, A. F. Tuck, G. C. Toon, M. R. Gunson, W. A. Traub, D. G. Johnson, K. W. Jucks, R. Zander, and I. G. Nolt, 1996b: Validation of hydrogen fluoride measurements made by the Halogen Occultation Experiment from the UARS platform. *J. Geophys. Res.,* **101,** 10 163–10 174.

Sarkissian, A., H. K. Roscoe, D. J. Fish, M. Van Roozendael, M. Gil, H. B. Chen, P. Wang, J.-P. Pommereau, and J. Lenoble, 1995a: Ozone and NO_2 air-mass factors for zenith-sky spectrometers: Intercomparison of calculations with different radiative transfer models. *Geophys. Res. Lett.,* **22,** 1113–1116.

——, ——, and ——, 1995b: Ozone measurements by zenith-sky spectrometers: An evaluation of errors in air-mass factors calculated by radiative transfer models. *J. Quant. Spectrosc. Radiat. Transfer,* **54,** 471–480.

Solomon, S., A. L. Schmeltekopf, and R. W. Sanders, 1987: On the interpretation of zenith sky absorption measurements. *J. Geophys. Res.,* **92,** 8311–8319.

Stolarski, R. S., P. Bloomfield, R. D. McPeters, and J. R. Herman, 1991: Total ozone trends deducted from Nimbus 7 TOMS data. *Geophys. Res. Lett.,* **18,** 1015–1018.

Taalas, P., and E. Kyrö, 1992: Two years of regular ozone soundings in the European Arctic, Sodankylä. *J. Geophys. Res.,* **97,** 8093–8097.

Torres, O., Z. Ahmad, and J. R. Herman, 1992: Optical effects of polar stratospheric clouds on the retrieval of TOMS total ozone. *J. Geophys. Res.,* **97,** 13 015–13 024.

Van Roozendael, M., M. De Mazière, and P. C. Simon, 1994: Ground-based visible measurements at the Jungfraujoch Station since 1990. *J. Quant. Spectrosc. Radiat. Transfer,* **52,** 231–240.

——, and Coauthors, 1995: Ground-based measurements of stratospheric OC1O, NO_2 and O_3 at Harestua, Norway (60°N, 10°E) during SESAME. *Proc. 12th ESA Symp. on European Rocket and Balloon Programmes and Related Research,* Lillehamer, Norway, ESA, 305–310.

——, P. Peeters, H. K. Roscoe, H. De Backer, A. Jones, G. Vaughan, F. Goutail, J.-P. Pommereau, E. Kyro, C. Wahlstrom, G. Braathen, and P. C. Simon 1998a: Validation of ground-based UV-visible measurements of total ozone by comparison with Dobson and Brewer spectrophotometers. *J. Atmos. Chem.,* **29,** 55–83.

——, and Coauthors, 1998b: Ground-based validation of GOME total ozone measurements by means of Dobson, Brewer and GUV instruments. *Atmospheric Ozone—Proceedings of the 18th Quadrennial Ozone Symposium,* R. D. Bojkov and G. Visconti, Eds., Vol. II, 665–668.

Vaughan, G., H. K. Roscoe, L. M. Bartlett, F. O'Connor, A. Sarkissian, M. Van Roozendael, J.-C. Lambert, P. C. Simon, K. Karlsen, B. A. Kaestad Hoiskar, D. J. Fish, R. L. Jones, R. Freshwater, J.-P. Pommereau, F. Goutail, S. B. Andersen, D. G. Drew, P. A. Hughes, D. Moore, J. Mellqvist, E. Hegels, T. Klupfel, F. Erle, K. Pfeilsticker, and U. Platt, 1997: An intercomparison of ground-based UV-visible sensors of ozone and NO_2. *J. Geophys. Res.,* **102,** 1411–1422.

WMO, 1995: Report of the tenth WMO international comparison of Dobson spectrophotometers. Environmental Pollution Monitoring and Research Programme Report Series 108, 19 pp.

Zander, R., P. Demoulin, E. Mahieu, G. P. Adrian, C. P. Rinsland, and A. Goldman, 1994: ESMOS II/NDSC IR spectral fitting algorithms intercomparison exercise. *Proceedings of the Third Conference on Atmospheric Spectroscopy Applications,* A. Barbe and L. Rothman, Eds., 7–12.